8 February 1996

PHYSICS LETTERS B

ELSEVIER

Physics Letters B 368 (1996) 259–265

Multifragment production in Au+Au at 35 MeV/u

Multics / Miniball Collaboration

M. D'Agostino [a], P.F. Mastinu [a], P.M. Milazzo [a], M. Bruno [a], D.R. Bowman [g], P. Buttazzo [b], L. Celano [c], N. Colonna [c], J.D. Dinius [f], A. Ferrero [d,h], M.L. Fiandri [a], C.K. Gelbke [f], T. Glasmacher [f], F. Gramegna [e], D.O. Handzy [f], D. Horn [g], W.C. Hsi [f], M. Huang [f], I. Iori [d], G.J. Kunde [f], M.A. Lisa [f], W.G. Lynch [f], L. Manduci [a], G.V. Margagliotti [b], C.P. Montoya [f], A. Moroni [d], G.F. Peaslee [f], F. Petruzzelli [d], L. Phair [f], R. Rui [b], C. Schwarz [f], M.B. Tsang [f], G. Vannini [b], C. Williams [f]

[a] *Dipartimento di Fisica and INFN, Bologna, Italy*
[b] *Dipartimento di Fisica and INFN, Trieste, Italy*
[c] *INFN, Bari, Italy*
[d] *Dipartimento di Fisica and INFN, Milano, Italy*
[e] *INFN, Laboratori Nazionali di Legnaro, Legnaro, Italy*
[f] *NSCL, Michigan State University, East Lansing, MI, USA*
[g] *Chalk River Laboratories, Chalk River, Ontario, Canada*
[h] *C.N.E.A., Buenos Aires, Argentina*

Received 27 July 1995; revised manuscript received 17 November 1995
Editor: R.H. Siemssen

Abstract

Multifragment disintegration has been measured with a high efficiency detection system for the reaction Au + Au at E/A = 35 MeV. From the event shape analysis and the comparison with the predictions of a many-body trajectories calculation the data, for central collisions, are compatible with a fast emission from a unique fragment source.

The disassembly of highly excited systems remains an open problem in the investigation of intermediate energy nucleus-nucleus collisions [1,2]. One of the challenging questions for head-on collisions is whether light particles and fragments emission is compatible with the fast emission from a unique thermalized source or it can still be explained in the deep-inelastic framework.

Several recent experimental studies of central collisions, performed with very heavy nuclei at different incident energies, give different indications on this point [3–6]. In 100 MeV/u Au + Au [3] central collisions, dynamical and statistical analyses [7] suggest that the large multiplicities, observed for light particles and intermediate mass fragments, are compatible with the prompt multifragmentation of a heavy, thermalized composite system with freeze-out density $\approx \frac{1}{3}-\frac{1}{6}$ of the normal nuclear density ($\rho_0 = 0.15$ fm^{-3}), even if the fragment probability emission resulted strongly influenced by the radial flow [3,8]. In the nearly symmetric Pb+Au reaction at 29 MeV/u [4] the charged products emission, studied for increasing neutron mul-

SSDI 0370-2693(95)01473-X

tiplicity, shows that the emission of intermediate mass fragments becomes the largest component of the cross section at the expense of projectile like fragments and fission fragments emission. On the other hand an analysis, mainly based on the event shape, of the same reaction Pb+Au [5,9] at the same incident energy seems to reveal that, even selecting the most central collisions, the largest part of the total reaction cross section is due to strongly damped binary collisions. Other studies on light particle and fragment emission [6] seem to confirm that, even selecting the most central collisions, the Incomplete Fusion cross section vanishes when reactions involving heavy projectile and targets at incident energies greater than ≈ 35 MeV/u are studied.

In this Letter we report the results of the analysis of central collisions for the reaction Au + Au at 35 MeV/u , measured with a high efficiency detection system. We will show that the observed fragment emission is compatible with the fast emission from a unique equilibrated intermediate nuclear system.

The experiment was performed at the National Superconducting Cyclotron Laboratory of the Michigan State University. Beams of Au ions at $E/A = 35$ MeV incident energy, accelerated by the K1200 cyclotron, were used to bombard Au foils of approximately 5 mg/cm^2 areal density. Light charged particles and fragments with charge $Z \leq 20$ were detected at $23° \leq \theta_{lab} \leq 160°$ by 159 phoswich detector elements of the MSU *Miniball* [10]. Reaction products with charge $Z \leq 83$ were detected at $3° \leq \theta_{lab} < 23°$ by the *Multics* array [11]. The charge identification thresholds were about 2, 3, 4 MeV/u in the *Miniball* for $Z = 3$, 10, 18, respectively and about 1.5 MeV/u in the *Multics* array independent of the fragment charge. The geometric acceptance of the combined apparata was greater than 87% of 4π.

From the total charged particle multiplicity N_c the reduced impact parameter $\hat{b}$ was determined, following Ref. [12]. Additional high statistics measurements were done using a shield, covering $\theta_{lab} < 8°$ in order to minimize the radiation damage of the most forward detectors[1]. In this way more than 10^5 events were collected for a centrality cut $N_c > 24$, $\hat{b} \leq 0.3$, which selects 10% of the total measured reaction cross section. In this range of impact parameters the measured light particles ($Z \leq 2$) multiplicity M_l has a mean value ~ 20 and the fragment ($Z > 2$) multiplicity N_f distribution has a gaussian shape with mean value 5.6 and standard deviation 1.8. The mean value of M_l is very much higher than the one chosen in Ref. [5] ($M_l > 10$) to identify the central collisions. The requirement $M_l > 10$, corresponding to $N_c > 15$, would select an impact parameter range $\hat{b} \leq 0.6$. Moreover the gaussian N_f distribution looks very different from the distribution shown in Fig. 2 of Ref. [5], where the two-fragments events represent the largest part of the measured cross section.

To investigate the fragment emission patterns we first performed a shape analysis, looking at the sphericity, coplanarity and flow angle, variables sensitive to the dynamics of the fragmentation process [13]. The emission of fragments from a unique source should be on the average isotropic in momentum space and the event shape should fluctuate around a sphere. Conversely in peripheral reactions the forward-backward emission of fragments from the spectator-like sources should lead to an event shape elongated along the beam axis, to a decrease of the sphericity value and to flow angles peaked in the forward direction.

In this analysis only events satisfying the constraint that at least 70% of the incoming momentum had been detected, were considered. For central and intermediate impact parameters, where the particle and fragments detection is less influenced than in peripheral collisions by the energy thresholds and the angular acceptance, a further constraint on the total detected charge (70% of the total charge) was applied.

The momentum tensor has been evaluated:

$$T_{ij} = \Sigma \frac{p_i^{(n)} \cdot p_j^{(n)}}{p^{(n)}} \quad (i,j = 1,2,3) , \tag{1}$$

where $p_i^{(n)}, p_j^{(n)}$ are the ith and jth cartesian projections of the momentum $\boldsymbol{p}^{(n)}$ of the nth fragment in the centre of mass frame. The sum runs over the number of fragments ($Z > 2$) detected in each event. The diagonalization of the flow tensor gives three eigenvalues λ_i and three eigenvectors $\boldsymbol{e}_i$. The event shape is an oriented ellipsoid with the principal axes parallel to the eigenvectors. The sphericity and coplanarity variables are, respectively, defined as

$$S = 1.5 \cdot (1 - \lambda_1) , \quad C = \tfrac{1}{2}\sqrt{3} \cdot (\lambda_2 - \lambda_3) , \tag{2}$$

[1] The shield was thick enough to stop the scattered Au ions.

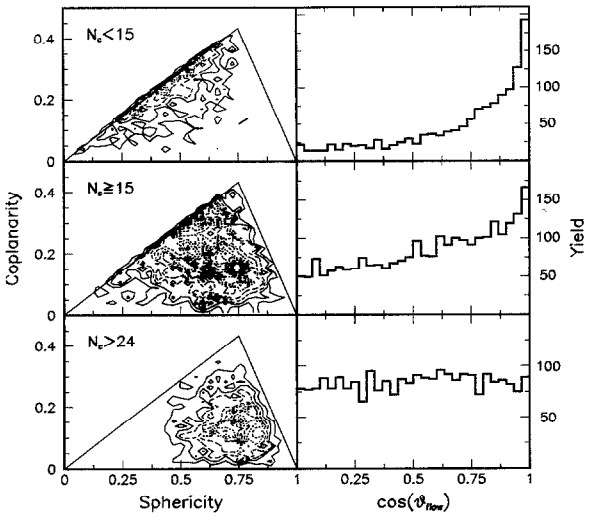

Fig. 1. Experimental sphericity-coplanarity linear contour plot and $\cos(\theta_{\text{flow}})$. Upper panels: $N_c < 15$ ($\hat{b} > 0.6$), intermediate panels: $N_c \geq 15$ ($\hat{b} \leq 0.6$), lower panels: $N_c > 24$ ($\hat{b} \leq 0.3$).

where $\lambda_1, \lambda_2, \lambda_3$ are the ordered eigenvalues ($\lambda_1 \geq \lambda_2 \geq \lambda_3$), normalized to their sum. The flow angle θ_{flow} is the angle between the eigenvector $\boldsymbol{e}_1$ for the largest eigenvalue λ_1 and the beam axis:

$$\cos(\theta_{\text{flow}}) = \boldsymbol{e}_1 \cdot \hat{k}. \tag{3}$$

Events with more than two detected fragments were used in the event shape analysis: two-body events, indeed, correspond mainly to peripheral reactions and do not give significant information, being two of the three eigenvalues zero for the momentum conservation.

In Fig. 1 the S–C plot is shown, together with the cosine of the flow angle for three different gates on N_c. For $N_c < 15$ which corresponds to $\hat{b} > 0.6$, as expected for peripheral events, the memory of the entrance channel dominates: one or two of the three eigenvalues extracted from the momentum tensor are nearly 0, so that the event is *pencil* or *disk* shaped and $\cos(\theta_{\text{flow}})$ is peaked in the forward direction. With a rough constraint on the centrality, i.e. requiring N_c larger than 15 ($\hat{b} \leq 0.6$), the events do not show a well defined shape, though the centroid of the events is shifted, with respect to the more peripheral collisions, towards the corner which represents spherical events. This behaviour reflects in the $\cos(\theta_{\text{flow}})$ distribution, which is less forward peaked than in the previous case. A more stringent constraint on the centrality ($N_c > 24$, $\hat{b} \leq 0.3$) leads to a drastic change of the S–C pattern: in these collisions the eigenvalues are very similar to each other, so that mainly events with shape close to a sphere are clearly present and $\cos(\theta_{\text{flow}})$ is randomly distributed, as expected in the case of fragments emitted from a unique source. Taking into account the modifications of the event shape with the requirement on the centrality and considering that the applied criterion on the total detected parallel momentum and the total charge does not eliminate the heavy residues, if they exist, we can deduce that the contribution from deep inelastic reactions is negligible at such small impact parameters [14].

The next step of the shape analysis consisted in the comparison of the experimental mean values $\langle S \rangle$ and $\langle C \rangle$ and their standard deviations ΔS, ΔC with the prediction of a many-body trajectory calculation [15], which has as basic assumption the uniqueness of an emitting system with zero angular momentum.

The experimental data considered in the following were selected with the centrality cut $N_c > 24$ ($\hat{b} \leq 0.3$). In the simulation both charge and energy of the reaction products are selected by randomly sampling the experimental single-particle yield for this cut. The fragments are emitted from a spherical source of radius R_s and charge Z_s. The individual emission time for each fragment is assumed to follow an exponential probability distribution, characterized by a decay constant τ. The emission is isotropic in the reference frame of the emitting system. A possible collective radial expansion can be accounted for by a further parameter v_{coll}, which allows to increase the fragment velocity by a component $\boldsymbol{v}(\boldsymbol{r}) = v_{\text{coll}}\boldsymbol{r}/R_s$, which attains its maximum value at the surface R_s of the source. The simulated events were treated in the same way as the experimental data, after filtering [16] them with the geometrical acceptance, granularity, energy thresholds and finite energy and angular resolutions. In our case, due to the mass symmetry in the entrance channel, the fragment source is at rest in the centre of mass frame. This give the advantage that no hypothesis is needed on the source velocity (on the percentage of the momentum transfer) contrary to the case of asymmetric reactions [17], when calculating the laboratory fragment velocities.

The comparison between $\langle S \rangle, \langle C \rangle$ is significant and represents a check of the compatibility between

the experimental observables and the decay of a unique source, provided that a set of input parameters (Z_s, R_s, τ, v_{coll}) is found, reproducing the fragment momenta used in Eq. (1) to build the momentum tensor. To this aim we performed several calculations, varying in a wide range the input parameters. For each set the predicted fragment emission velocities as a function of the emission angle and the fragment reduced velocity correlation functions have been compared to the experimental data. The experimental N_c, N_f and Z_{bound} (total charge bound in form of fragments with $Z > 2$) spectra were continuously used to keep under control the reasonability of the predictions.

We found that a source with charge $\approx$ 86% of the total charge (Z_s = 138), freeze-out density $\sim \rho_0/4$ (radius R_s = 13 fm), which emits the fragments with an average time between successive fragment emissions [9] $\tau \approx 85$ fm/c reproduces the previously mentioned observables, provided that an expansion radial velocity $\approx$ 1.4 cm/ns is taken into account. As can be seen in Figs. 2a–2c the experimental distributions of the fragment emission velocities as a function of the emission angle θ_{cm} are very well reproduced, irrespective of the selected fragment charge, even at forward and backward centre of mass angles, most affected by the experimental acceptance.

Since the isotropy of the fragment emission, assumed by the calculation, implies that the emission velocity, for a given fragment charge, is constant over the whole range of θ_{cm}, we investigated more in detail the main reasons of the rise of the experimental distribution at small centre of mass angles and of the dip at backward θ_{cm}. It is important indeed to understand whether these distortions can be ascribed to the boost of sources not at rest in the centre of mass or they are only due to experimental limitations. A simple kinematical calculation showed that, starting from a constant emission velocity with gaussian profile (in the calculation of Fig. 2d) 3 cm/ns with standard deviation 1 cm/ns), the combined effects of the laboratory angular and velocity acceptance do not sharply cut the spectrum but they select at the most forward (backward) angles the highest (lowest) values of the velocity distribution. In particular the enhancement at $\theta_{cm} <$ 50° is mainly due to the forward angular limitation and the dip at $\theta_{cm} >$ 130° to the velocity thresholds. For $\theta_{cm} \approx$ 50°–130° the distribution is only slightly affected by the experimental limitations, so that the mean value in this angular range corresponds to the *true* emission velocity. For sake of comparison we report in Fig. 2d) the experimental emission velocity for fragments with Z = 6, which have in the θ_{cm} range 50°–130° a mean emission velocity $\sim$ 3 cm/ns.

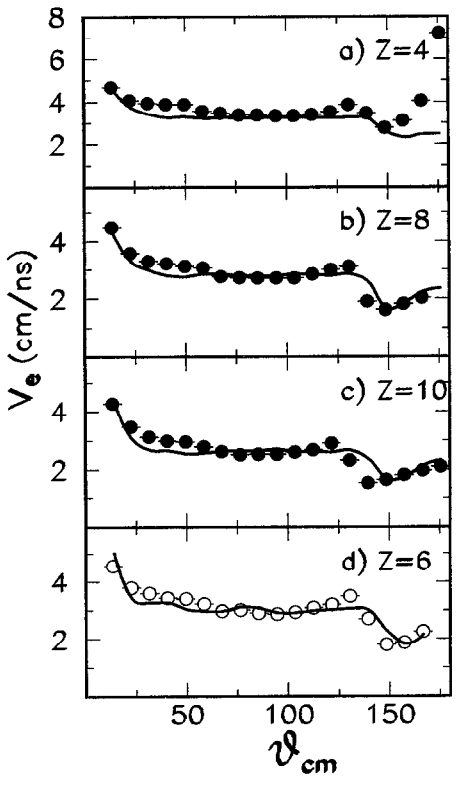

Fig. 2. (a), (b), (c): Experimental emission velocities (points) for fragments with charge 4, 8 and 10, compared with the many-body trajectory calculations (line). The statistical experimental error is smaller than the size of the points. (d) Experimental emission velocities for fragments with charge 6 (open points) compared with a constant emission velocity (3 cm/ns with standard deviation 1 cm/ns) (line) filtered with the constraints 8° $\leq \theta_{lab} \leq$ 160°, $v_{threshold}$ = 1.5 cm/ns ($\theta_{lab} <$ 23°), $v_{threshold}$ = 2.5 cm/ns ($\theta_{lab} \geq$ 23°).

The reproduction of the relative fragment momenta was then checked through the comparison of the two-fragments correlation functions. The shape of the correlation function at small values of the reduced velocities is a measure of the spatial separation of the emitted fragments and is therefore sensitive to the input parameters of the calculation.

The correlation functions [18,19] were calculated by

$$1 + R = C\frac{Y(v_{red})}{Y_{mix}(v_{red})}, \quad (4)$$

where v_{red} is the reduced velocity of fragments i and j ($i \neq j$) (charges Z_i and Z_j):

$$v_{red} = \frac{|\, v_i - v_j \,|}{\sqrt{(Z_i + Z_j)}}. \quad (5)$$

$Y(v_{red})$ and $Y_{mix}(v_{red})$ are the coincidence and mixed yields for fragment pairs of reduced velocity v_{red}. The mixed yield was constructed by means of the mixing event technique, C is a normalization factor fixed by the requirement to have the same number of true and mixed pairs [18].

We analyzed separately fragments detected in the *Multics* array and in the *Miniball*, since the solid angle covered by the apparata is very different and an average on the whole solid angle would lead to a loss of information. From Figs. 3a, 3b (fragments detected in *Multics*) and Figs. 3c, 3d (fragments detected in the *Miniball*) one can see that the many-body trajectories code well reproduces the experimental correlation functions, irrespective of the selected fragment charge, assuming an average time between successive fragment emissions τ = 85 fm/c and a collective radial expansion $v_{coll} \approx 1.4$ cm/ns. Varying τ by some tens of fm/c the experimental correlation functions are not so well reproduced: the decreased or increased distance among the emitted fragments introduces additional correlations or anticorrelations, respectively, not present in the data [20]. It has to be noted that the experimentally observed *Coulomb hole* at small values of the reduced velocity leads to the same choice of the parameter τ both in the case of fragments emitted at small relative angles (detected in *Multics*) and in the case of fragments emitted at large relative angles (detected in the *Miniball*). In addition in the first case the selection of τ can be performed by checking even the reproduction of the enhancement of the correlation function at $v_{red} \approx 20$. This bump, due to the mutual Coulomb repulsion between the closely emitted partners (see Figs. 3a and 3b), is sensitive to the increase of the proximity of the fragments induced by the decrease of τ.

The small value found for the radial collective velocity, although consistent with the extrapolation to 35 MeV/u of data at higher energies [21], should be thoroughly investigated before making any conclusion. It could be ascribed either to the assumption of non overlapping fragments or to the schematic treatment of the Coulomb component: a change of the emission geometry, which reflects in an increase of the fragment Coulomb energy, could compensate the need of a radial expansion. Furthermore in a recent theoretical work [22] on the effect of the angular momentum on the statistical fragmentation, it was found that a rotation mechanism could explain some features

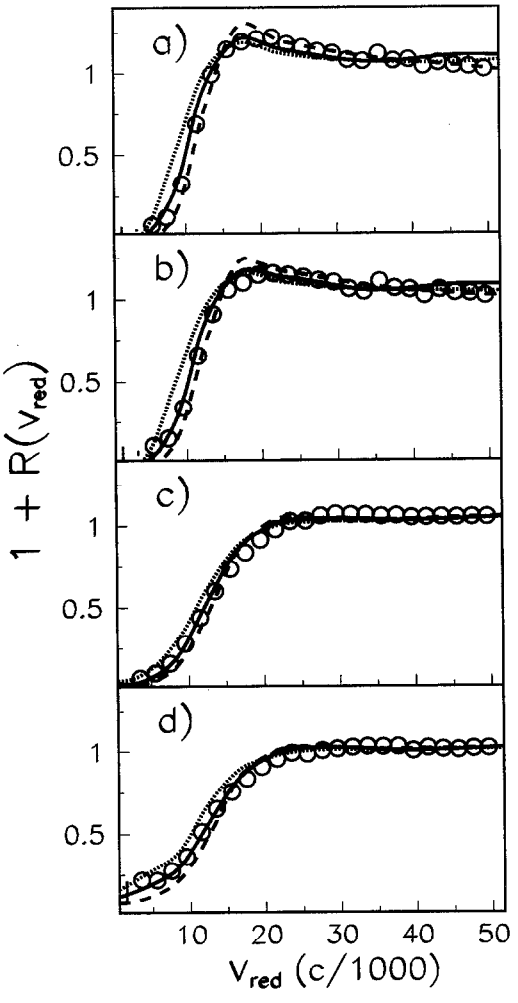

Fig. 3. Two fragment correlation functions for: (a) $3 \leq Z_{IMF} \leq 30$ and $8° \leq \theta_{lab} < 23°$, (b) $3 \leq Z_{IMF} \leq 20$ and $8° \leq \theta_{lab} < 23°$, (c) $3 \leq Z_{IMF} \leq 20$ and $23° \leq \theta_{lab} \leq 160°$, (d) $3 \leq Z_{IMF} \leq 10$ and $23° \leq \theta_{lab} \leq 160°$. Open points show experimental data. The solid, dashed and dotted lines are the the many-body trajectory predictions for τ = 85, 50, 150 fm/c, respectively.

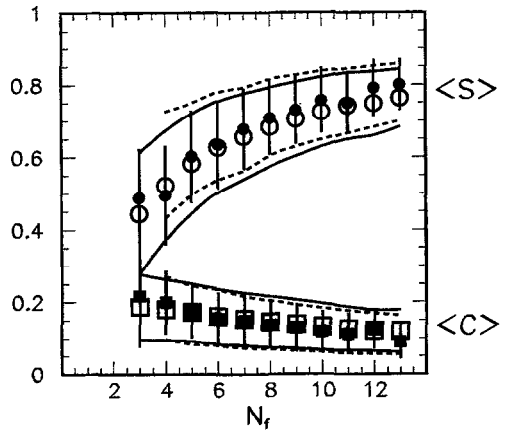

Fig. 4. Mean sphericity $\langle S \rangle$ and coplanarity $\langle C \rangle$ and their standard deviations ΔS, ΔC as a function of N_f. Experimental $\langle S \rangle$, $\langle C \rangle$, ΔS, ΔC are reported as full symbols and vertical bars, respectively. $\langle S \rangle$, $\langle C \rangle$ calculated from the filtered predictions are reported as open symbols and $\langle S \rangle \pm \Delta S$, $\langle C \rangle \pm \Delta C$ as full lines. $\langle S \rangle \pm \Delta S$, $\langle C \rangle \pm \Delta C$ from the unfiltered predictions are shown by dashed lines.

previously ascribed to a collective flow of the nuclear matter. The comparison to predictions of statistical models which take into account either the radial flow or the angular momentum for systems with mass of some hundreds of nucleons should be performed, but this is beyond the aim of this Letter.

Since the observed fragment emission patterns are well reproduced by the many-body trajectory calculation, the comparison between experimental and predicted $\langle S \rangle$, $\langle C \rangle$ and their standard deviations ΔS, ΔC as a function of the fragment multiplicity becomes significant to draw a conclusion on the compatibility of our data with the uniqueness of the decaying system. From Fig. 4 the very good agreement between data and predictions is evident, not only for $\langle S \rangle$, $\langle C \rangle$, but even for the standard deviations ΔS, ΔC, irrespective of the selected fragment multiplicity. Observing the unfiltered predictions (dashed lines in Fig. 4), we can deduce that the effects of the experimental inefficiencies very slightly decrease $\langle S \rangle$ and increase $\langle C \rangle$. Moreover events with $N_f = 3$, not present in the unfiltered predictions, are only few percent both in the experimental data and in the filtered predictions. We would like to stress that this agreement is not a trivial consequence of the reproduction of the fragment multiplicity. Indeed even in the case of peripheral collisions (Fig. 1a)) events with fragment multiplicity up to 7 were measured, but in this case the forward-backward emission flattens the fragment momenta into a plane and $\langle S \rangle$ and $\langle C \rangle$ reveal *pencil/disk* shaped events.

In conclusion, for the central collisions of the reaction Au + Au at $E/A = 35$ MeV, the good agreement among the measured observables and the predictions of a many-body trajectories code confirms both the assumptions on the uniqueness of the fragment source and on the isotropy of the fragment emission.

This work has been supported in part by funds of the Italian Ministry of University and Scientific Research. The technical assistance of R. Bassini, C. Boiano, S. Brambilla, G. Busacchi, A. Cortesi, M. Malatesta and R. Scardaoni during the measurements is gratefully acknowledged.

References

[1] See, for instance, L.G. Moretto and G.J. Wozniak, Ann. Rev. Nucl. Part. Sci. 43 (1993) 379, and references quoted therein.
[2] Sa Ban-Hao and D.H.E. Gross, Nucl. Phys. A 437 (1985) 643;
J.P. Bondorf et al., Nucl. Phys. A 443 (1985) 321; A 444 (1985) 460.
[3] W.C. Hsi et al., Phys. Rev. Lett. 25 (1994) 3367;
G.J. Kunde et al., Phys. Rev. Lett. 24 (1995) 38.
[4] E. Piasecki et al., Phys. Rev. Lett. 66 (1991) 1291.
[5] J.F. Lecolley et al., Phys. Lett. B 325 (1994) 317.
[6] J.C. Steckmeyer et al., XXXIII Intern. Winter Meeting on Nuclear Physics (Bormio, January 1995), ed. I. Iori, Ric. Sci. and E.P. 101 (1995) 183;
E. De Filippo, et al.,XXXIII Intern. Winter Meeting on Nuclear Physics (Bormio, January 1995), ed. I.Iori, Ric. Sci. and E.P. 101 (1995) 217;
V. Metivier et al., XXXIII Intern. Winter Meeting on Nuclear Physics (Bormio, January 1995), ed. I. Iori, Ric. Sci. and E.P. 101 (1995) 255.
[7] J.P. Bondorf et al., Phys. Rev. Lett. 73 (1994) 628.
[8] S.C. Jeong et al., Phys. Rev. Lett. 72 (1994) 3468;
G. Poggi et al., Nucl. Phys. A 586 (1995) 755.
[9] D. Durand et al., Phys. Lett. B 345 (1995) 397.
[10] R.T. DeSouza et al., Nucl. Instrum. Methods A 295 (1990) 109.
[11] I. Iori et al., Nucl. Instrum. Methods A 325 (1993) 458;
M. Bruno et al., Nucl. Instrum. Methods A 311 (1992) 189;
N. Colonna et al., Nucl. Instrum. Methods A 321 (1992) 529;
P.F. Mastinu et al. Nucl. Instrum. Methods 338 (1994) 419.
[12] C. Cavata et al. Phys. Rev. C 42 (1990) 1760;
M.B. Tsang et al., Phys. Rev. Lett. 71 (1993) 1502.
[13] J. Cugnon and D. L'Hote, Nucl. Phys. A 397 (1983) 519.

[14] M. D'Agostino et al., XXXIII Intern. Winter Meeting on Nuclear Physics (Bormio, January 1995), ed. I. Iori, Ric. Sci. and E.P. 101 (1995) 237;
M. D'Agostino et al., Phys. Rev. Lett. (1995), in press.
[15] T. Glasmacher et al., Phys. Rev. C 50 (1994) 952.
[16] M. Bruno et al., Nucl. Instrum. Methods A 305 (1991) 410.
[17] P. Danielewicz, Phys. Rev. C 51 (1995) 716.
[18] R. Trockel et al., Phys. Rev. Lett. 59 (1987) 2844.
[19] D.R. Bowman et al., Phys. Rev. Lett. 70 (1993) 3534;
M. Aboufariassi et al., XXXII Intern. Winter Meeting on Nuclear Physics (Bormio, January 1994), ed. I. Iori, Ric. Sci. and E.P. 97 (1994) 1;
R. Bougault et al., Ric. Sci. and E.P. 97 (1994) p. 28.
[20] O. Schapiro and D.H.E. Gross, Nucl. Phys. A 573 (1994) 143; A 576 (1994) 428.
[21] W. Reisdorf et al., Proc. Intern. Workshop XXII (Hirschegg, 1994), eds.H. Feldmeier and W. Nörenberg, p. 93.
[22] A.S. Botvina and D.H.E. Gross, Nucl. Phys. A 592 (1995) 257.